Knowledge-Based IMRT Treatment Planning for Bilateral Head and Neck Cancer

by

Matthew Charles Schmidt

Graduate Program in Medical Physics
Duke University

Date:_____

Approved:

_____
Shiva K. Das, Co-Supervisor

_____
Joseph Y. Lo, Co-Supervisor

_____
Robert Reiman Jr.

Thesis submitted in partial fulfillment of
the requirements for the degree of Master of Science in the
Graduate Program in Medical Physics in the Graduate School
of Duke University

2013

ABSTRACT

Knowledge-Based IMRT Treatment Planning for Bilateral Head and Neck Cancer

by

Matthew Charles Schmidt

Graduate Program in Medical Physics
Duke University

Date:_____
Approved:

_____
Shiva K. Das, Co-Supervisor

_____
Joseph Y. Lo, Co-Supervisor

_____
Robert Reiman, Jr.

An abstract of a Thesis submitted in partial
fulfillment of the requirements for the degree
of Master of Science in the
Graduate Program in Medical Physics in the Graduate School of
Duke University

2013

Abstract

Intensity-modulated radiotherapy (IMRT) remains the standard of care for external beam radiation therapy for head and neck cancers. Planning for IMRT requires a trial-and-error approach that is completely dependent on planner expertise and time available for multiple iterations of manual optimization adjustments. Knowledge-based radiation therapy planning utilizes a database of previously planned Duke University Medical Center patient plans to create clinically comparable treatment plans by comparing the geometrical two-dimensional projections of the planning target volume (PTV) and organs at risk (OAR). These 2D beam's eye view (BEV) images are first aligned with squared error registration, then the similarity is computed using the mutual information (MI) metric. After the closest match is found, computed constraints and deformed fluence maps are entered into Eclipse treatment planning system to generate the new knowledge-based treatment plan. For this study, 20 randomly selected cases were matched against a database of 103 head and neck cancer cases. The resulting new plans were compared to their clinically planned counterparts. For these 20 cases, 13 proved to be dosimetrically comparable by evaluation of the PTV dose-volume histogram. In 92% of cases planned, at least half of the OARs were also deemed comparable or better than the original plan. These cases were planned in less than 25

minutes with no manual constraint objective adjustments, as opposed to many hours needed in clinical planning.

Dedication

I dedicate my thesis to my parents for their unwavering support and to Laura Lynn Walsh for choosing sacrifice so that I may savor more happiness.

Contents

List of Tables

List of Figures

Acknowledgements

I would like to thank Dr. Lo and Dr. Das for their guidance throughout this project. I would also like to thank David Good and Deon Dick for helping to lay the foundation for which this algorithm is based.

1. Introduction

Head and neck cancers are defined by the National Cancer Institute as any cancer that affects the head or neck region[1]. This includes the nasal and oral cavities, tongue, lips, throat, mouth and larynx, but excludes the brain, eye, esophagus, thyroid, as well as the scalp, skin, muscles, and bones of the region[1]. In the US, it is estimated that over 52,000 new cases of head and neck cancers were expected to arise in the year 2012, resulting in more than 11,000 deaths[2]. Head and Neck cancers can be organized into bilateral, unilateral right, and unilateral left (figure 1).

Figure 2: Examples of Head and Neck cancers. From left to right: Bilateral, Unilateral Left, and Unilateral Right.

A standard approach to treatment for these cases includes local approaches, such as surgery and radiation therapy, with the addition of chemotherapy in some exceptions. In advanced stage cancers, it is preferable to combine treatment modalities[3]. Patients with early stage disease retain cure rates of 80 percent or more[4, 5].

Intensity modulated radiation therapy (IMRT) has remained the standard choice of external beam radiation therapy for years with head and neck cancers[6-9]. This type of

radiation treatment provides much better sparing of organs at risk (OAR) while allowing for an escalation of dose to the target, or planning target volume (PTV). In order to accomplish this feat, the intensity pattern within each beam of radiation is altered throughout the treatment. This type of target conformation is essential for such concise treatment needs[6]. IMRT has been shown to improve the quality of life for patients undergoing therapy by sparing the critical organs surrounding the tumor, including the parotid glands, thereby reducing xerostomia when compared to conformal RT[10, 11]. Other complications that may result from external beam radiation in the head and neck region consist of speech disorder, dysphagia, pain, and depression[12]. IMRT surpasses 3D conformal treatment with better tumor coverage and OAR sparing, but it requires stricter immobilization methods to confirm the radiation is being delivered to the correct calculated regions[8]. With the use of IMRT, 3-year survival can surpass 80 percent[5].

The planning for these treatments is typically developed *de novo*, with the doses optimized in a trial-and-error fashion[13, 14]. This type of treatment can take an experienced planner several hours to achieve acceptable optimization goals. The quality of the treatment plans depends heavily on user experience and time available for multiple iterations of optimization computations. It has been shown that more experienced treatment planners create superior IMRT plans, providing evidence for the reliance of

expertise of the planner[15]. This knowledge-based method also ensures the propagation of high quality plans. Plan variability remains an existing problem among IMRT treatment plans with head and neck plans—possessing more dose deviation from prescribed dose than prostate and brain cancers according to Das, et al.[16] Methods have been proposed at improving the plan quality of IMRT treatments such as generating a dose-volume histogram based on the spatial similarity and dosimetric properties of previously planned patients[17-19].

The healthy organs at risk that will be considered in this study are the left and right parotids, brainstem, oral cavity, spinal cord, and larynx (figure 2). Other OARs include the pharynx, mandible, etc., but these will not be included in this study. In order to ensure sparing of the spinal cord, a margin is typically added to the contoured structure[7, 20]. Duke University Hospital adds a 5mm margin to the spinal cord for possible patient positioning and motion errors.

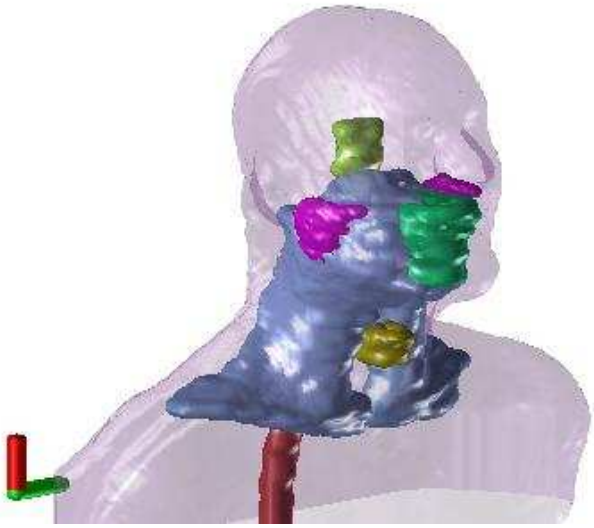

Figure 3: 3D image of the body with PTV (blue), Left and right Parotids (purple), Brainstem (green), Oral Cavity (turquois), Larynx (gold), and Spinal Cord with 5mm margin (red).

Head and neck cases generally require 7-9 beams in order to deliver a substantial dose to the PTV while sparing the OARs. At Duke University Hospital, for bilateral cases, nine angles are used (figure 3). These angles begin at a PA beam and rotate around the body in 40 degree increments (180°, 140°, 100°, 60°, 20°, 340°, 300°, 260°, and 220°).

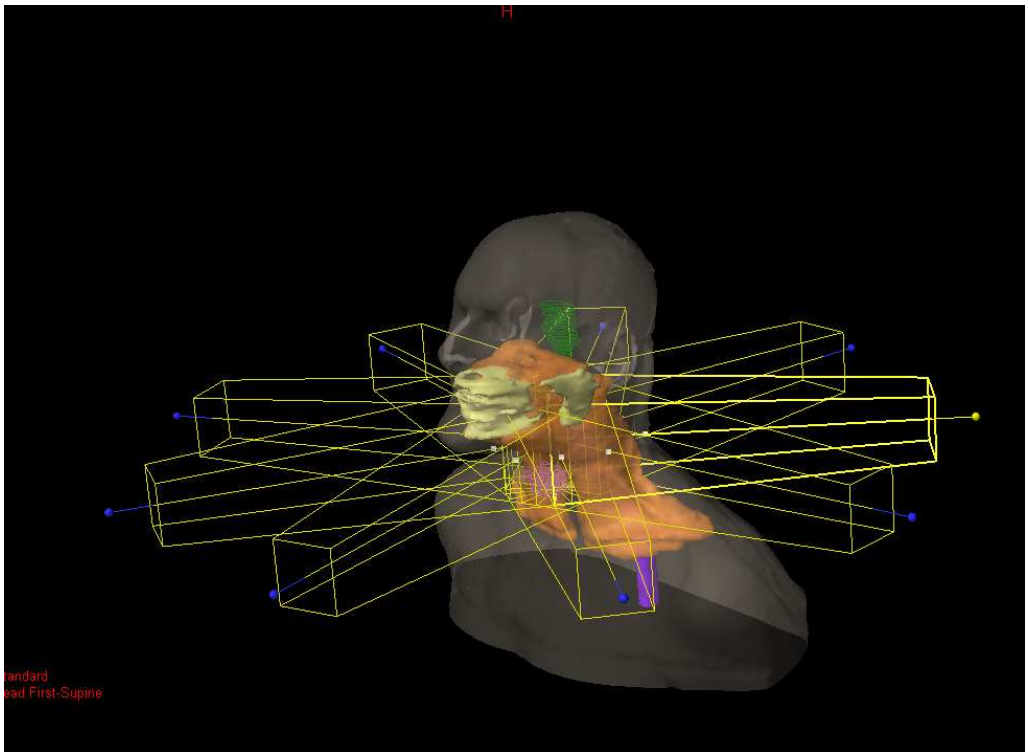

Figure 4: 3D image of the 9 treatment beams in a head and neck case. Created with Eclipse treatment planning software.

The dose optimization produces radiation map for each beam aperture. The intensity at any point in the beam aperture is proportional to the length of time that the radiation is allowed to pass through that point. In order to compare the plan quality of these cases, a dose volume histogram (DVH) is generated. The cumulative DVH shows the percentage of a structure's volume that receives a total amount of a certain dose.

Previous approaches to knowledge based IMRT treatment planning have shown promising results in reducing the amount of time needed to create a treatment plan without sacrificing significant quality in the plan[13,21,22]. Previous KBRT work has

investigated the application of knowledge-based treatment planning to prostate cancers. This study of knowledge-based IMRT for head and neck, as a more complicated treatment site, posed some unique challenges. For instance, in prostate tumors, the planning target volume is much more uniform on a case by case basis, whereas the head and neck PTVs are significantly variable (in both size and shape) between patients. Many of these bilateral head and neck PTVs are also much larger than the prostate. There are also more critical structures being considered; the prostate planning had 4 OARs (right and left femoral heads, bladder, and rectum) while the plans being reviewed in this paper use 6. The purpose of this study is to demonstrate that this knowledge-based approach of matching a patient geometry with a library of previously planned cases can result in a comparable plan at a fraction of the time spent with the trial-and-error method of optimization currently used.

2. Methods and Materials:

2.1 Knowledge Base

From March 2012 to February 2013, 103 head and neck cancer patients were used for the knowledge base library, including 62 with bilateral tumors. Once these anonymized cases were extracted from Eclipse Treatment Planning System (version A10, Varian Medical Systems, Palo Alto, CA), they were converted into structured MATLAB (Mathworks, Natick, MA) files using the Computational Environment for Radiotherapy Research (CERR)[23].

The standard of care at our institution is described below. The PTV was constructed from the Clinical Target Volume (CTV) with the addition of a 3mm margin. The organs at risk were the parotid glands, oral cavity, larynx, brainstem, and spinal + 5mm margin for further critical structure sparing. The nine (9) treatment beams were oriented at the angles of 20°, 60°, 100°, 140°, 180°, 220°, 260°, 300°, and 340° per Duke University Medical Center's (DUMC) standard. All beams were delivered at 6MV with the optimization constraints customized for each individual patient.

A patient chosen from this knowledge base is denoted the "query" case. This case is handled as if no dosimetric information regarding the treatment of this patient is available. In this study, 20 query cases were chosen, and with each chosen query case, the remaining 102 cases served as potential "match" cases from the knowledge base.

2.2 Two-Dimensional Projection and Alignment

In brief, the knowledge-based approach for treatment planning involves extracting the query patient's anatomical structures and converting them into 2D projections. The projections are compared with mutual information to find the closest anatomical match. The match case fluence are deformed to fit the query patient's scaled PTV, and this new information is imported into Eclipse treatment planning system for optimization, using constraints that are adopted from the closest match case.

Eclipse treatment planning system exports the anatomical information, which was then imported into CERR to represent the structures as 3D images. Since the query case will adopt the same treatment beam angles as the match case, it is sufficient to compare the anatomic geometry of these cases as a set of 2 dimensional projections of the beam's eye view (BEV) images (figure 4) for each of the beams . Masks of the PTV superimposed with the OARs were created.

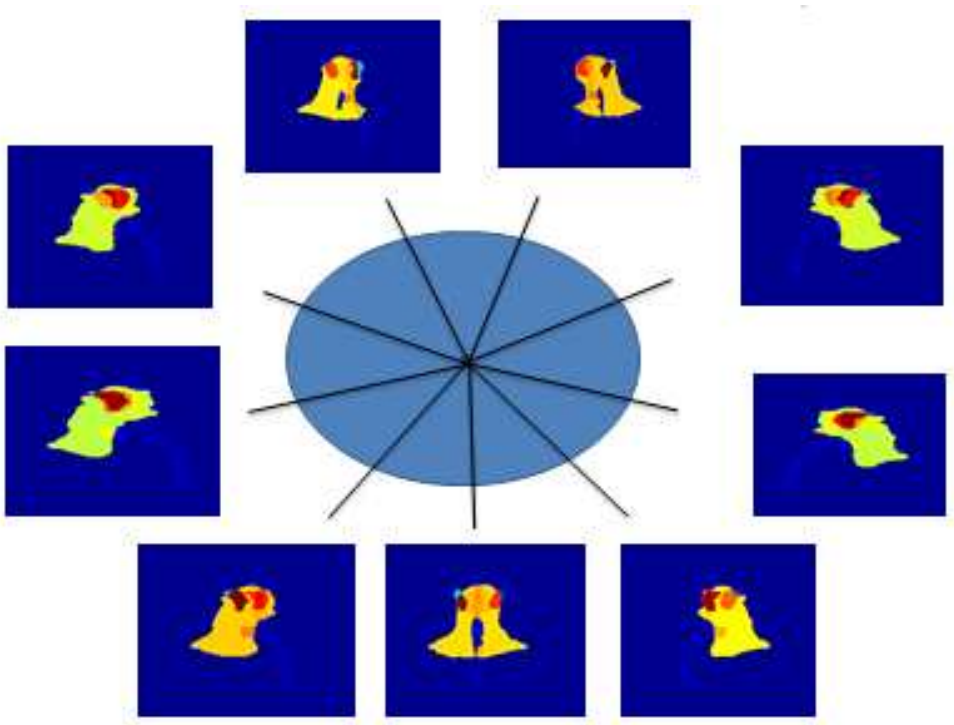

Figure 5: BEVs of the superimposed masks containing the PTV with the OARs

Due to the large variation in PTVs, the CERR code was edited to create a consistent cm-to-pixel ratio of the 3D images[21].

Before our similarity metric is applied, the images are properly aligned to yield optimal results. Binary BEV images of only the PTV were generated from the PA beam (angle 180°), then the match image is translated using the gradient descent of a least squared error (equation 1) measurement to align with the query image.

The minimum value for this equation corresponds to most similarly matched images, where $I_{i,j}^{moving}$ is shifted along the target image, $I_{i,j}^{target}$, in order to find a minimum value. Figure 5 shows the difference in images before and after this translated shifting. This shift is recorded and all other organs are translated by the same amount.

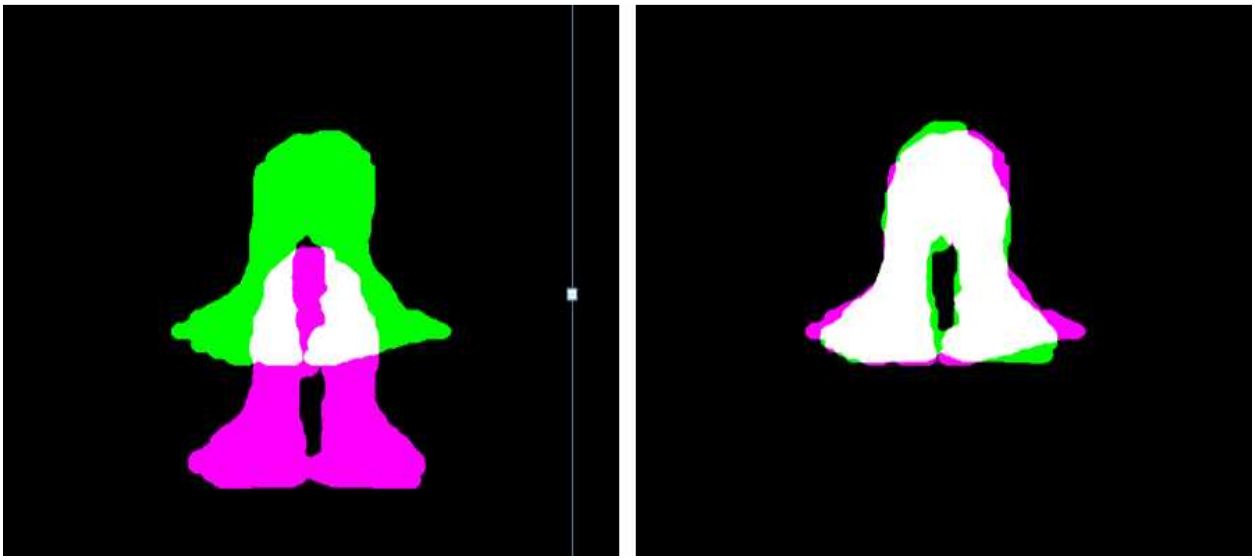

Figure 6: The unregistered query BEV image with the best match (left). The same BEVs shifted using the mean square error are ready for the similarity metric (right).

The squared error is preferred for this pre-registration because of its computational speed[24,25]. Given each query case, the squared error metric was also used to identify the top 12 potential matches in the database. This process tended to rule out the unilateral tumor cases and highly dissimilar bilateral cases, saving computational time and memory when applying the similarity metric.

2.3 Scaling and Similarity Metric:

Once the PTV and other organs were properly aligned onto the query patient, the BEV images were assigned pixel values using a binary counting scheme, such that each structure or overlapping combination of structures had a unique value. Customary to clinical practice at our institution, to minimize dose in the back and shoulders, the inferior portion of the field angles for 100°-260° (figure 6) are restricted so their inferior margins are above the shoulders. Since the fluence fields do not encompass the lower portion of these PTVs at these angles, the BEVs are scaled to the approximate ratio of these fluence maps.

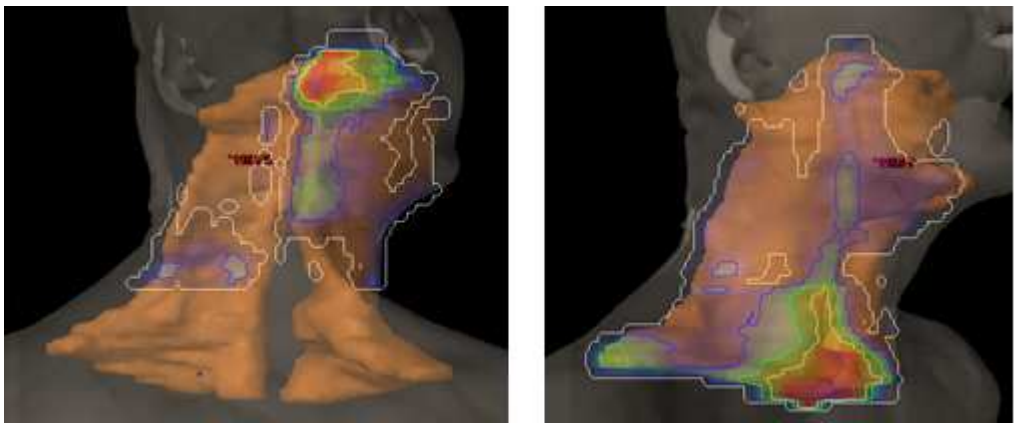

Figure 7: Beam restriction shown in a clinically planned case to avoid dose to the shoulders, back and lungs. The left image is a more posterior image while the right image is anterior. Note: These two images correspond to angle 140 (right) and 60 (left)

In order to accomplish this scaling, proportions are created from the height of the match case PTV BEV and fluence map. A "scale factor" is created and applied to the query case

in order to recreate this calculated ratio from the match case. From figure 7, it is discernible that this scale factor allows for the BEV image to be more open at the anterior angles. The similarity metric is applied to these combined structure images that have been scaled down.

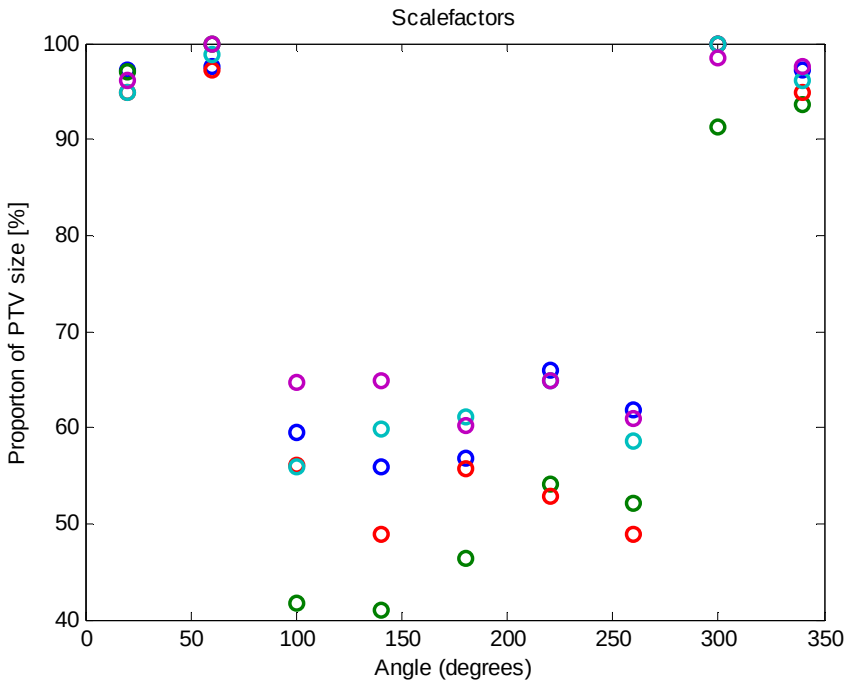

Figure 8: The scale factors at different angles for five match cases. Notice the anterior angles (20°, 60°, 300°, and 340°) are relatively open compared to the lateral/posterior beams.

Figure 8 shows an example of an open field beam and a limited field beam when the scale factor is applied. These scaled images are used in the similarity metric for two reasons. One reason is to determine where the inferior collimator jaw should be placed during the treatment planning process. Another reason for this scaling is to ensure that

the similarity metric is only applied to the portion of the structure geometry where there is fluence—the images applied to the similarity metric are the images on the right side of figure 8.

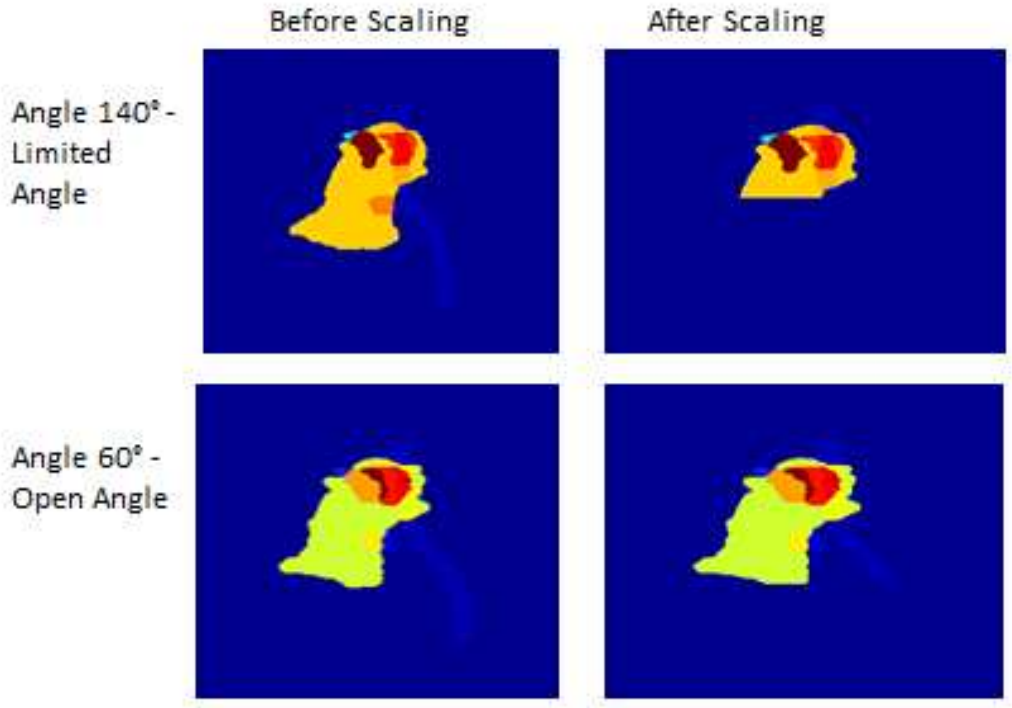

Figure 9: Mask BEV images with and without the scaling factor applied. Some image angles (top) require a significant scaling factor to reduce dose through the shoulders and back while others (bottom) maintain a more open field.

The similarity of these two cases was calculated using mutual information (MI). The metric, which increases with the statistical dependency between two data sets, was calculated for each case as the average MI over all BEV angle projections. The mutual information between the query and match image projections for each BEV can be calculated by equation 2.

$$MI(A,B) = \sum_{i_a,i_b} P_{AB}(i_a,i_b)\log_2\left(\frac{P_{AB}(i_a,i_b)}{P_A(i_a)P_B(i_b)}\right) \quad (2)$$

In this equation images are labeled A and B, i_a is the intensity level in image A, i_b is the intensity level in image B. P_A and P_B are the probabilities of intensities i_a and i_b occurring in images A and B respectively. P_{AB} represents the probability that the intensity level in image A, i_a , will be represented in the same pixel by the intensity level in image B, i_b. The match patient with the highest average MI score over all beam angles was concluded to have the most geometric similarity to the query patient.

2.4 Registration, Deformation and Constraint Calculation

Although the MI metric identified the match case with the most similar anatomy, the fluences for that case would not be inherently optimal for the query case. In order to tailor the match case beam fluences to the query case, the match fluences must be deformed to fit the PTV area. Elastix[26] was used to deform the match case fluences through a multi-pass b-spline registration process. Elastix created a deformation map to distort the match PTV to fit on the query; this deformation map was then applied to the match fluence for conformal adjustments (figure 9). These transformed parameters were saved to be used in the planning of the new treatment.

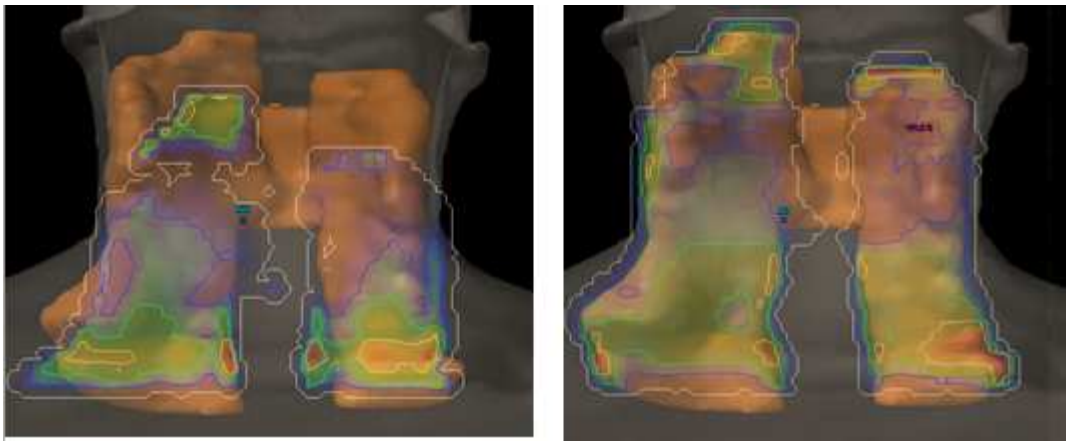

Figure 10: The match fluence before deformation using Elastix on the left, and after deformation on the right. Both were superimposed onto the query PTV

Critical structure constraints for the query case were calculated in MATLAB. In order to calculate these constraints, the dose distribution and the volumes of each individual structure were extracted from the match plan. The dose distribution for the match plan was deformed and mapped onto the query case, such that query and match points with the same distance from the PTV were assigned the same dose (figure 10). This mapped dose distribution was used to generate an expected dose-volume histogram for the query case. The dose constraints for the query structures were extracted from the created DVH and defined at 40% and 60% volume for the oral cavity, larynx, and parotids and at 0% volume (maximum dose) for the spinal cord and brainstem. These objectives were dependent on volume of the structure, the overlap with the PTV, and the dose distribution of the match case.

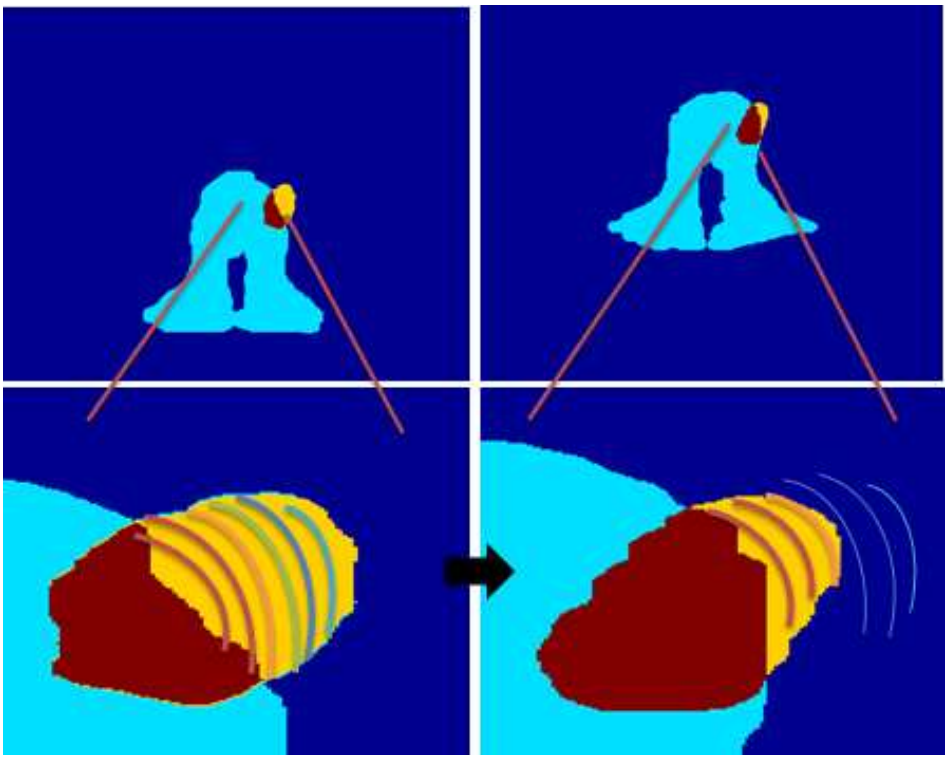

Figure 11: The match plan (top left) possesses a dose distribution (bottom left) that is deformed and mapped onto the query case (top right) to create a new dose distribution (bottom right) for the constraint calculation.

2.4 Plan Creation and Evaluation

The optimal deformed fluences from Elastix were imported into Eclipse treatment planning system. The plan was created with identical beam angles and constraint weights as the match case (note that the dose-volume constraints are generated as explained in the previous section). The jaw sizes for the beams were fit around the PTV with a 1cm margin at angles 20°, 60°, 300°, and 340°; the other angles employ the same fitting, but the inferior jaw was moved up to the bottom of the fluence

map to reduce the amount of radiation passing through the shoulders and back. Anisotropic Analytical Algorithm (AAA), a pencil beam superposition convolution, is used in Eclipse dose calculations. The optimization process utilizes the constraints calculated in MATLAB from the match case parameters. Dose fall-off away from PTV in non-organ normal tissue is specified as in the match case. The PTV default objective of 101.5% and 98.5% were used for the upper and lower PTV constraint respectively. During the optimization, no modifications were made to any plan parameters, i.e., the optimization was allowed to proceed with no manual intervention until the results reached an asymptote.

DVH information was exported from Eclipse and analyzed in MATLAB. The oral cavity, larynx, and parotids were evaluated based on their mean and median values in the DVH, while the brainstem and spinal cord were assessed by their maximum dose. The maximum dose was defined as the dose at a volume of 1%. The query case plan generated with the method used here, denoted "KBRT", was examined in contrast with the actual clinically generated plan, denoted "original". These plans were considered comparable if their mean and median doses or maximum doses were within 5% of the original case.

The PTV of the original and KBRT plans were compared by evaluating the Homogeneity Index (HI) and S_index (equation 3 and 4) for each plan[27]. HI measured

the steepness of the slope of the PTV DVH. The S_index measured the deviation from the mean PTV dose.

$$HI = \frac{D_2 - D_{98}}{D_p} x\ 100\% \qquad (3)$$

$$S_{index} = \sqrt{\sum (D_i - D_{mean})^2 * \frac{v_i}{V_{total}}} \qquad (4)$$

D_2 and D_{98} were the doses at 2% and 98% volume of the PTV, respectively. D_p was the prescribed dose. D_i was the dose within the volume v_i; D_{mean} was the average dose in the PTV, and V_{total} was the total volume of the PTV. The maximum dose was also calculated by extracting the dose at a volume of 1% from the DVH. The mean, median, maximum doses, homogeneity index, and S_index were all compared to the original plan using the percent difference (equation 5). These doses are portrayed as a percentage of the prescription dose.

$$\%difference = \frac{Dose_{original}(\%) - Dose_{KBRT}(\%)}{Dose_{original}(\%)} * 100 \qquad (5)$$

The Wilcoxon signed rank test was used to determine the statistical significance of the dose differences in both the OARs and PTV when comparing the KBRT versus original plans. This signed rank test is a non-parametric assessment of the dependency of two similar data sets.

The time to complete the image registration, and fluence deformation is approximately 12-14 minutes. The amount of time to upload these fluences into Eclipse

and create a completely new plan using this information takes about 5 minutes, and 100 iterations of optimization utilizes another 5 minutes. None of these steps require any user judgment or decision making. Therefore treatment plans are created in a semi-automated manner in less than 25 minutes.

3. Results

3.1 OAR and PTV Evaluation

There are many ways to analyze the dosimetric plan quality. The dose volume histogram (DVH) allows the user to assess the volume of the structure above each dose level. This graphical summary of dose distribution was used to analyze each OAR. In each case, the DVH of the KBRT plan was compared to that of the clinical plan. The left and right parotids, the oral cavity and the larynx were evaluated on their mean and median doses, computed from the DVH. The spinal cord and brainstem were evaluated for the maximum dose (taken here as the dose to 1% volume) delivered to the organ. These metrics for KBRT and original plans, the percent differences and the p value from the Wilcoxon signed rank test are listed in table 1.

Table 1: The mean and median doses for the parotids, larynx, and oral cavity and the maximum doses at 1% volume for the spinal cord and brainstem taken from the DVH. The percent difference and Wilcoxon signed rank p values are also tabulated. Positive percent difference implies KBRT had higher dose than original.

Organ (N = 20 Cases)	Mean/median or max (%)	Original (% of prescription)	KBRT (% of prescription)	%difference	P value
Left Parotid	Mean	53.23 ± 17.9	54.33 ± 10.4	2.08	0.67
	Median	46.78 ± 27.1	44.84 ± 15.9	-4.15	0.77
Right Parotid	Mean	48.14 ± 13.9	47.01 ± 9.9	-2.36	0.53
	Median	40.38 ± 20.0	34.77 ± 12.2	-13.88	0.53
Larynx	Mean	54.38 ± 18.0	56.43 ± 15.7	3.77	0.30
	Median	50.24 ± 19.6	50.79 ± 17.7	1.10	0.91
Oral Cavity	Mean	57.48 ± 9.5	56.90 ± 9.4	-1.01	0.70
	Median	52.48 ± 10.5	51.11 ± 9.4	-2.61	0.72

Spinal Cord	Max	61.73 ± 8.0	58.13 ± 3.5	-5.83	0.07
Brainstem	Max	33.94 ± 11.8	30.55 ± 9.7	-9.98	0.03

In Table 1, the KBRT performance for almost all OARs was comparable. Although doses to left parotids and larynx were slightly worse for the KBRT algorithm, those differences were not significant. The only significant difference was for the brainstem, where KBRT was slightly better.

Table 2 lists the PTV max dose, HI and S-index. An HI value less than 15 is considered clinically acceptable, as is a PTV maximum dose of less than 115%. As seen here, the maximum KBRT PTV dose was close to that from the original case and less than 115% (although the difference was statistically significant, the values are not clinically significantly different). The HI for the KBRT cases was less than 15. Although statistically significant, the percent differences for the HI and S_index between the KBRT and original cases were also clinically small.

Table 2: PTV evaluation of original and KBRT plans using the max dose, the homogeneity index, and the S_index.

PTV Metrics (20 Cases)	Original (% of prescription)	KBRT (% of prescription)	%difference	P value
Max dose (%)	109.14 ± 1.7	110.21 ± 1.7	0.98	0.0015
Homogeneity Ind.	10.24 ± 2.1	10.91 ± 2.1	6.49	0.05
S_index	449.54 ± 20.5	459.35 ± 18.7	2.18	0.0045

3.2 Case Wide Evaluations

It is also useful to look how each case performs compared to the original case. Table 3 groups the cases according to the number of OARs (out of 6) that are either better (difference was negative) or comparable (difference was positive but less than 5%). For the 20 cases analyzed, 17 of them had at least half of the OARs considered better or comparable. Figures (11-18) show the DVHs for 8 selected cases. In all figures, solid lines denote the original plan and dotted lines denote the KBRT plan.

Table 3: OAR comparison between KBRT and original plans.

Number of OARs that are better or comparable in the KBRT plan	Number of Cases
6 OAR better or comparable	1
5 OAR	5
4 OAR	6
3 OAR	5
2 OAR	3
1 OAR	0
All OAR worse	0

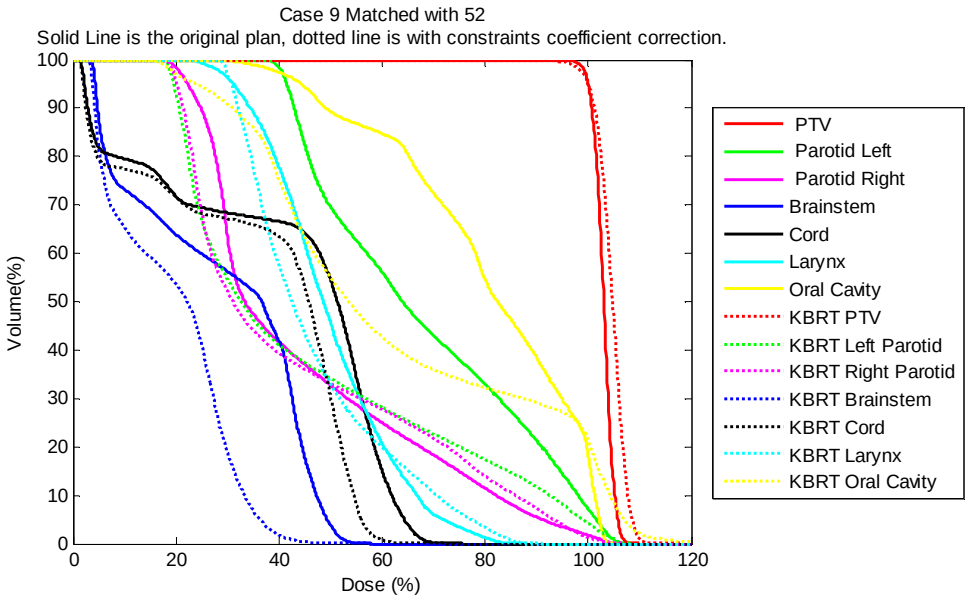

Figure 12: DVH for KBRT case 9 and match case 52. All OARs are better with the KBRT case than the original.

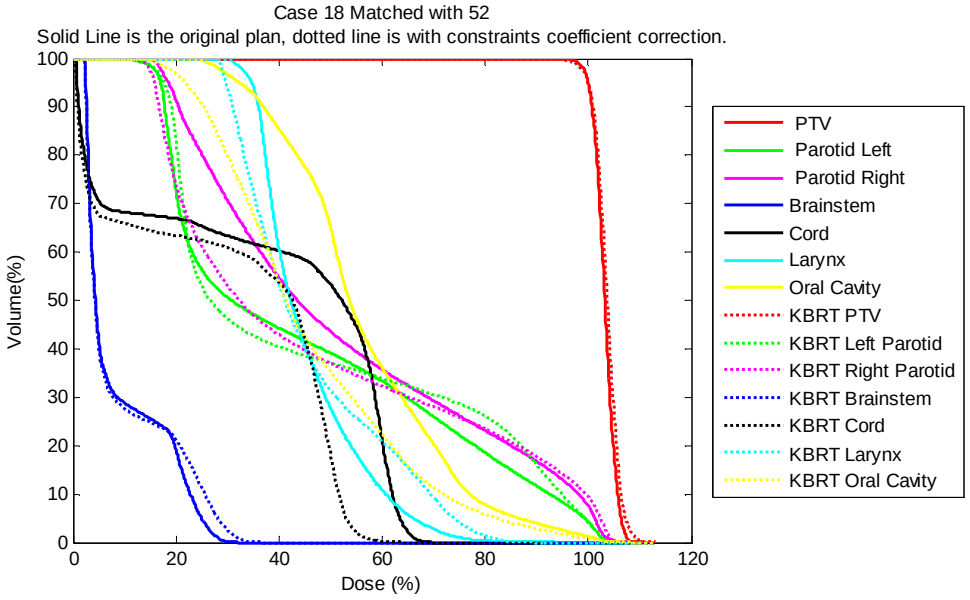

Figure 13: DVH for KBRT case 18 and match case 52. One OAR was higher (the brainstem maximum dose) when comparing KRT to original case.

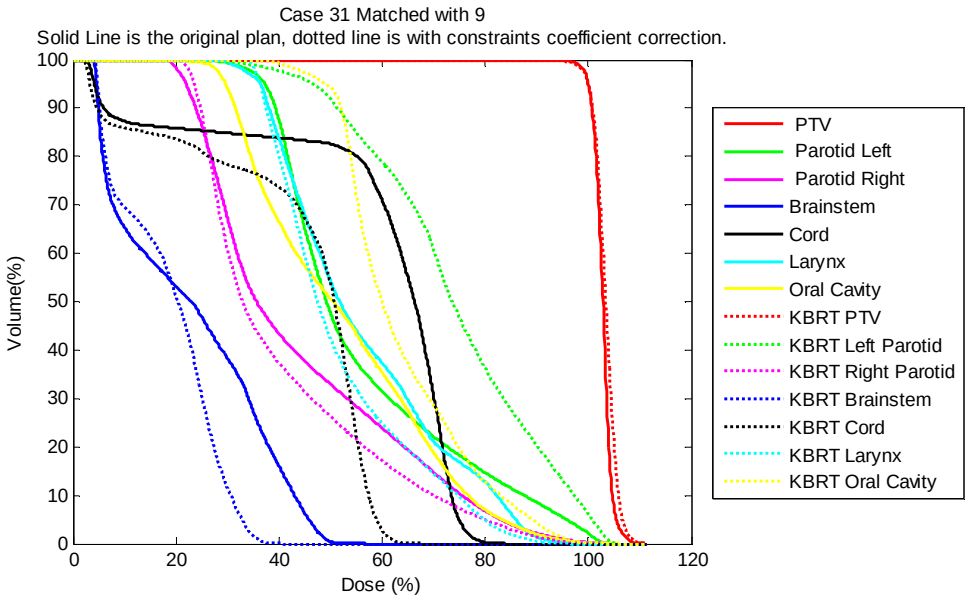

Figure 14: DVH of case 31 compared with match case 9. The left parotid and oral cavity were worse, but all other organs were comparable or better.

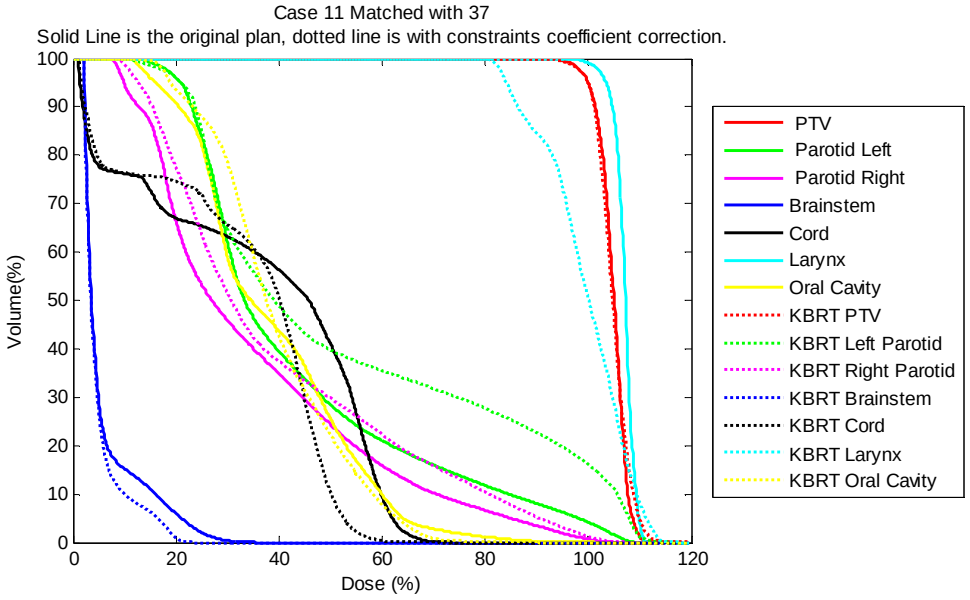

Figure 15: DVH of KBRT case 11 and match case 37. Half of the OARs were worse (left parotid, right parotid, and oral cavity) and the other half were better or comparable.

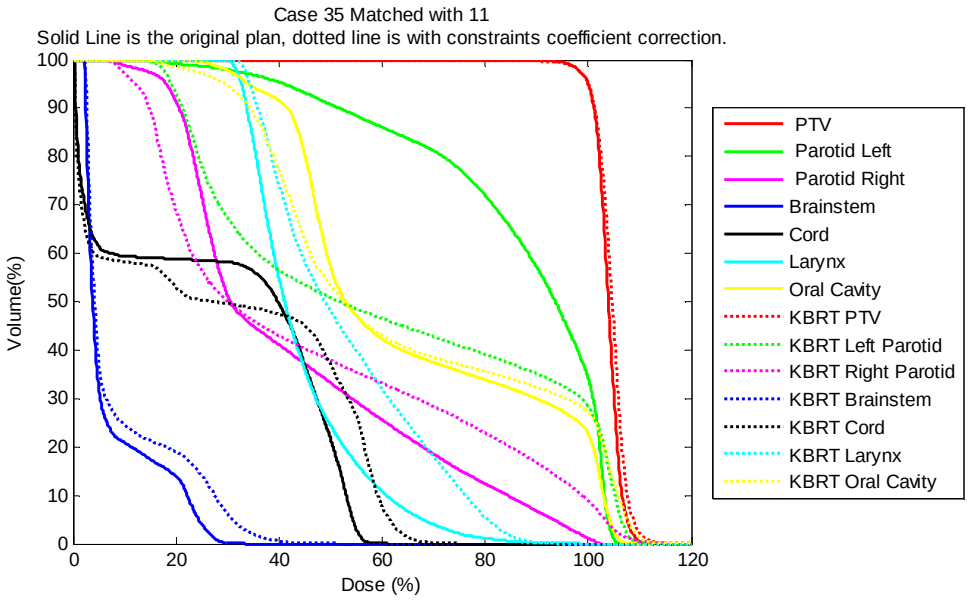

Figure 16: DVH of case 35 compared with match case 11. Only 2 OARs were better comparable (left parotid and oral cavity) while 4 others were worse.

Figure 15 is a peculiar case with an interesting feature. The clinically planned case does not have any constraints for the larynx. This can be seen from the high dosage given to the larynx in the DVH. With the KBRT plan, dose objectives are placed on every structure, so this helps pull this high larynx dose down. In a clinical world, where the dose should be as low as reasonably achievable (ALARA), these dose constraints can be beneficial to the patient.

3.3 Organ-at-risk Analysis:

The results were also compiled for individual organs. Table 4 displays the number of cases for which the KBRT DVH for a particular structure was better than that

for the original case. From this table, the left parotid has the least number of cases in which the KBRT was better, while all other structures were better in a majority of cases.

Table 4: Structure-based comparison between KBRT and original plans.

Structure	# cases in which this structure was better or comparable (20 cases total)
Left Parotid	9
Right Parotid	12
Larynx	11
Oral Cavity	13
Spinal Cord	15
Brainstem	16
PTV	13

4. Conclusions and Future Work

4.1 Discussion

The purpose of this knowledge-based IMRT treatment planning is to create plans of a comparable dosimetric quality to clinically planned cases. The benefits to the KBRT method is the amount of time saved for understaffed and overworked clinics, and most importantly the creation of high quality plans on a consistent basis. Based on this study, it is concluded that clinically similar plans can be created using this KBRT metric. When organ doses were compared between KBRT and original plans, nearly all differences

were small and not statistically significant. There was only one significant difference (brainstem), where the KBRT plan was actually better.

An examination of cases where the KBRT plan performed poorly for a particular structure did not reveal any obvious patters, e.g., extent of overlap between the PTV and structure. For these cases matched via mutual information metric, the PTV match dominates the MI score due to its much larger size than the OARs. This means that the best MI match for a query case may not be the best match for the organs at risk. To remedy this situation, each organ would need to be matched based on an individual structure MI score. This is discussed more in the Future Works section.

The PTV performed comparably overall between the KBRT and original cases. Although p values for the PTV metrics demonstrated statistical significance, the difference values for the maximum dose and the S_index are minor, and the HI is considered clinically because its value is below 15. Also, for every structure analyzed, all but one structure had better DVHs for the KBRT plan in a majority of cases. These trends show that the target homogeneity and healthy tissue sparing for the KBRT plan are comparable to the clinically planned cases. Similar trends were observed in previous studies applying a knowledge-based approach to prostate cancer IMRT treatment planning[13,21].

4.2 Future Work

This knowledge-based treatment planning algorithm is dependent on the number of treatment angles used throughout the treatment. Our institution utilizes a standard 9 beam treatment for bilateral head and neck cancers. In order to expand this project further, it would be beneficial to include unilateral left and unilateral right cases as well. The size of the match database should also be expanded and more query cases should be analyzed to allow more thorough statistical evaluation.

Currently the similarity metric is applied to an entire mask of the target projections superimposed with all of the OAR volumes. To fully optimize this, mutual information should be calculated for each organ-at-risk individually. This would allow for the matching of dose distributions specific to each structure, yielding more precise results in the dose-constraint creations. This may allow the merging of beneficial qualities from multiple cases in order to achieve an optimal treatment plan. Using a method such as this would also allow for the constraint calculations and comparisons to be created on an individual structure basis.

4.3 Conclusions:

IMRT treatment planning requires an abundance of time and expertise. The plan quality of each cancer therapy can be greatly affected from factors such as lack of experience, understaffing, or user error. This knowledge-based approach to planning

external beam radiation therapy uses two dimensional BEV data in order to deform a geometrically similar fluence map to the query patient PTV. This requires no manual intervention and is completely independent of user input—constraint objectives chosen, and optimization iterations allowed . This study analyzed 20 patients with a knowledge database of 103 patients, and determined that plans that are similar to the original clinically approved plan used to treat the patient could be created in a semi-automated process. This KBRT method used in the creation 20 planned cases show comparable results for many of the evaluations of the DVH. The PTV compared better or comparable in the majority of these cases. The OARs varied for individual structure ranging from a the lowest number and highest number of cases considered better or comparable than the clinically planned cases for the left parotid and brainstem respectively.

With further advancements in the methodologies of this treatment planning algorithm, KBRT treatment planning possesses the potential to provide comparable dosimetric quality plans for all head and neck tumor cases. As the knowledge-base continues to grow to include more variations in organ and tumor geometry, head and neck IMRT treatment planning using this technique will improve in quality.

References

1 National Cancer Institute. *Head and Neck Cancer*. The National Institute of Health; Available from: http://www.cancer.gov/cancertopics/types/head-and-neck.

2 American Cancer Society, *Cancer Facts & Figures 2012.* 2012.

3 Shah, Jatin P. and Lydiatt, William, *Treatment of Cancer of the Head and Neck.* CA Cancer J Clin 1995; 45(6): p. 352-368.

4 Vokes, E, et al., *Head and Neck Cancer*. N Engl J Med 1993; 328: p. 184-194.

5 Yoa, M. et al., *Intensity-modulated radiation treatment for head-and-neck squamous cell carcinoma—The University of Iowa experience.* Int J of Rad Onc Biol. Phys., 2005; 63(2): p. 410-421.

6 Lee, N., et al., *Intensity Modulated Radiation Therapy for Head-And-Neck Cancer: The UCSF Experience Focusing on Target Volume Delineation.* Int J of Rad Onc Biol. Phys., 2003; 57(1): p.158-168.

7 Purdy, James, *Current ICRU Definitions of Volumes: limitations and Future Directions.* Semin Radiat Oncol. 2004; 14(1): p. 27-40.

8 Huang, D., et al., *Comparison of Treatment Plans Using Intensity-Modulated Radiotherapy and Three-Dimensional Conformal Radiotherapy for Paranasal Sinus Carcinoma.* Int. J. Radiation Oncology Biol. Phys., 2003; 56(1): p. 158-168.

9 Chao, K. S. C., et al., *Intensity-Modulated radiation therapy in head and neck cancers: The Mallinckrodt experience.* Int J of Cancer, 2000; 90(2): p 92-103.

10 Lin, A., et al., *Quality of life after parotid-sparing IMRT for head-and-neck cancer: A prospective longitudinal study.* Int J of Rad Onc Biol. Phys., 2003; 57(1): p. 61-70.

11 Parliament, M., et al., *Preservation of oral health-related quality of life and salivary flow rates after inverse-planned intensity-modulated radiotherapy (IMRT) for head-and-neck cancer.* Int J of Rad Onc Biol. Phys., 2004; 58(3): p.663-673.

12 Nguyen, N., et al., *Combined chemotherapy and radiation therapy for head and neck malignancies.* Cancer 2002; 94(4): p. 1131-1141.

13 Chanyavanich, V., et al., *Knowledge-based IMRT treatment planning for prostate cancer.* Med Phys 2011; 38(5): p. 2515-2522.

14 Pugachev, A. et al., *Role of beam orientation optimization in intensity-modulated radiation therapy.* Int J of Rad Onc Biol. Phys., 2001; 50: p. 551-560.

15 Chung, H.T., et al., *Can all centers plan Intensity-Modulated Radiotherapy(IMRT) effectively? An external audit of the dosimetric comparisons between three-dimensional conformal radiotherapy IMRT for Adjuvant Chemoradiation for Gastic Cancer.* Int J of Rad Onc Biol Phys., 2008; 71(4): p. 1167-1174.

16 Das, Indra J., et al., *Intensity-Modulated Radiation Therapy Dose Prescription, Recording, and Delivery: Patterns of Variability Among Institutions and Treatment Planning Systems.* Journal of the National Cancer Institute, 2008; 100(5): p. 300-307.

17 Wu, B., et al., *Data-Driven Approach to Generating Achievable Dose-Volume Histogram Objectives in Intensity Modulated Radiatiotherapy Planning.* Int J of Rad Biol Phys., 2001; 79(4): p. 1241-1247.

18 Petit, S. F., *Increased organ sparing using shape-based treatment plan optimization for intensity modulated radiation therapy of pancreatic adenocarcinoma.*Radiotherapy and Oncology., 2012; 102(1): p. 38-44.

19 Xiaofeng Zhu, et al., *A planning quality evaluation tool for prostate adaptive IMRT based on machine learning.* Medical Physics, 2011; 38(719): p. 719-726.[20]Lee, S., et al., *Preliminary results of a phaseI/II study of simultaneous modulated accelerated radiotherapy for nondisseminated nasopharyngeal carcinoma.* Int J of Rad Onc Biol. Phys., 2006; 65(1): p 152-160.

21 Good, David, et al., *A Knowledge-based Approach to Improving Homogenizing Intensity Modulated Radiotherapy (IMRT) Planning Quality Among Treatment Centers: An Example Application of Prostate Planning.* Int J of Rad Biol Phys., 2013 (in press).

22 Dick, Deon, M.S., Knowledge-Based IMRT Treatment Planning for Prostate Cancer: Experience with 101 cases from Duke Clinic. Duke University Libraries. 2012; http://hdl.handle.net/10161/6187.

23 J.O., A.I. Blanco, and V.H. Clark, *Cerr, a computational environment for radiotherapy research,* Med Phys, 2003; 30: p. 979-985.

24 Zitova, Barbara, and Flusser, Jan, *Image registration methods: a survey.* Image and Vision Computing, 2003; 21(11): p. 977-1000.

25 Hill, D. L. G., et al., *Medical Image Registration*.Phys. Med Biol., 2001; 46 p. R1-R45.

26 Klein, S., et al., *Elastix: a toolbox for intensity based medical image registration.* IEEE Transitions in Medical Imaging, 2010; 29(1): p. 196-205.

27 Yoon, M., et al., *A new homogeneity index based on statistical analysis of the dose volume histogram.* J Appl Clin Med Phys, 2007; 8(2): p. 9-17.